Quaternary Geochronology 30 (2015) 213–218

Contents lists available at ScienceDirect

Quaternary Geochronology

journal homepage: www.elsevier.com/locate/quageo

Research paper

Single-grain and multi-grain OSL dating of river terrace sediments in the Tabernas Basin, SE Spain

M.R. Geach [a, *], K.J. Thomsen [b], J.-P. Buylaert [b, c], A.S. Murray [c], A.E. Mather [a], M.W. Telfer [a], M. Stokes [a]

[a] School of Geography, Earth and Environmental Sciences, Plymouth University, Drakes Circus, Devon PL4 8AA, UK
[b] Center for Nuclear Technologies, Technical University of Denmark, DTU Risø Campus, Denmark
[c] Nordic Laboratory for Luminescence Dating, Department of Geoscience, University of Aarhus, Risø Campus, Denmark

ARTICLE INFO

Article history:
Received 28 October 2014
Received in revised form
28 May 2015
Accepted 29 May 2015
Available online 10 June 2015

Keywords:
Fluvial
Tectonics
Climate
OSL

ABSTRACT

River terraces represent important records of landscape response to e.g. base-level change and tectonic movement. Both these driving forces are important in the southern Iberian Peninsula. In this study, Optically Stimulated Luminescence (OSL) dating was used to date two principal river terraces in the Tabernas Basin, SE Spain. A total of 23 samples was collected from the fluvial terraces for dating using quartz OSL. Sixteen of the samples could not be dated because of low saturation levels (e.g. typical $2xD_0 < 50$ Gy). The remaining seven samples (5 fossil and 2 modern analogues) were investigated using both multi-grain and single-grain analysis. Single grain results show that: (i) measurements from multi-grain aliquots overestimate ages by up to ~ 4 ka for modern analogues and young samples (<5 ka), presumably because (ii) the presence of many saturated grains has biased the multi-grain results to older ages. Despite the unfavourable luminescence characteristics we are able to present the first numerical ages for two terrace aggradation stages in the Tabernas Basin, one at ~16 ka and the other within the last 2 ka.

1. Introduction

In the Tabernas Basin southeast Spain, river terraces record basin-wide aggradational and incisional periods driven by external and internal forcing agents (e.g. tectonics, climate and lithological controls) throughout the Quaternary (Harvey et al., 2003; Nash and Smith, 2003). The Basin is one of a series of interconnected Neogene sedimentary basins located within the Internal Zone of the Betic Cordillera (Betics) (Fig. S1A). The Quaternary basin morphology records considerable variation in vertical incision over a lateral distance of ~12 km (Fig. S1B). In the east of the basin, the landscape is dominated by aggradational alluvial fans that record little incision (<10 m). In contrast, the central and western parts of the basin record up to 250 m of incision (i.e. vertical separation of current river bed and the uppermost Quaternary terrace surface), with the formation of a sequence of inset fluvial terraces (i.e. a river staircase; Alexander et al., 2008). The variation in basin incision is typically attributed to regional differences in tectonically-driven base-level change (Harvey, 2007). However, Harvey et al. (2003) suggest that climatic factors and further internal controls (e.g. variations in lithological strength) are also of significance in the delivery and routing of sediment both to, and within, the basin.

Unfortunately, due to the poor preservation of organic materials in the terrace record and the lack of application of other dating methods (e.g. luminescence, cosmogenic nuclide dating), little is known concerning the timing of major periods of changes in fluvial dynamics in the basin (Nogueras et al., 2000). In this study, we use quartz optically stimulated luminescence (OSL) to date fluvial samples obtained from two terrace levels in the Tabernas Basin. Quartz OSL was selected for investigation because of the ubiquity of quartz, and because quartz OSL is reset rapidly on exposure to daylight (e.g. Jain et al., 2004a). One of the key assumptions in OSL dating is that the signal was adequately reset at deposition, so that any residual signal is insignificant compared to the burial signal. If this is not the case, an OSL age based on standard multi-grain aliquots is likely to overestimate the depositional age, because of the presence of poorly-bleached grains (e.g. Olley et al., 1999).

One approach to identifying the likelihood of significant incomplete bleaching is to measure the doses recorded by very young or modern sediments (modern analogues; e.g. Murray and

* Corresponding author.
E-mail address: martin.geach@plymouth.ac.uk (M.R. Geach).

http://dx.doi.org/10.1016/j.quageo.2015.05.021
1871-1014/

Olley, 2002; Jain et al., 2004a; Vandenberghe et al., 2007; Porat et al., 2010; Murray et al., 2012). Here the assumption is that the recent sedimentary environment is analogous to that of the fossil samples, although such modern analogues are likely to be worst-case scenarios due to a low preservation potential (Jain et al., 2004a). The average multi-grain residual dose from young or modern quartz samples from fluvial and colluvial environments around the world is ~2 Gy (67 samples; Murray et al., 2012) indicating that in such environments incomplete bleaching is likely only to be of concern in relatively young samples (e.g. < 20 ka).

Another approach to identifying the potential for significant incomplete bleaching is to make use of the differential bleaching rates of quartz and feldspar luminescence signals; these signals bleach at very different rates (about one order of magnitude difference) and so by comparing quartz OSL and feldspar (post-IR) IRSL ages, it should be possible to determine whether a given quartz sample is likely to have been well-bleached at deposition (e.g. Murray et al., 2012). This approach of course requires the presence of suitable feldspar grains, which are not always common in mature sediments.

A third approach in identifying the likelihood of significant incomplete bleaching is to examine the characteristics of single-grain dose distributions, e.g. over-dispersion (OD; Galbraith et al., 1999) and skewness (Bailey and Arnold, 2006). However, Thomsen et al. (2012) have shown that over-dispersion is not a reliable indicator of incomplete bleaching, and Medialdea et al. (2014) found the decision tree model of Bailey and Arnold (2006) resulted in gross underestimations in six out of eight cases. In multi-grain dose distributions, incomplete bleaching is masked by averaging effects (depending on aliquot size and grain sensitivity), but if some of the grains were well-bleached at burial it is possible to identify these by analysing single-grain dose distributions using one of various minimum age models (e.g. review by Duller, 2008) and thus estimate the depositional age accurately.

The principal aim of this study is to use single-grain and multi-grain OSL techniques in order develop a framework chronology for the youngest river terrace levels in the Tabernas Basin. Here we present both multi-grain and single-grain quartz OSL ages of five fossil and two modern samples from a region with unfavourable OSL characteristics. The main reason for undertaking OSL measurement of the modern samples is to investigate whether it is likely that the fossil samples suffer from significant incomplete bleaching. This dataset provides a valuable basis for the development and application of OSL techniques to the Tabernas Basin and other similar regions in southern Iberia.

2. Sample details and experimental procedures

Four levels of Quaternary inset terraces were identified as common across the Tabernas Basin (Fig. S2; Geach et al., 2014). These occur at ~80 m (level 1: oldest), ~50 m (level 2), ~30 m – 10 m (level 3) and <5 m (level 4: youngest) above the current channel (Fig. 1A). The sedimentology of the terraces indicates deposition in laterally-extensive alluvial fans for terrace levels 1 and 2 with a later shift to more confined, braided fluvial styles for levels 3 and 4.

Sampling for OSL dating was limited due to the highly indurated nature and coarse grain size (gravel dominated) of most exposures. A total of 23 samples were collected from the fluvial staircase, including two modern analogue samples. No samples were collected from terrace level 1 due to the hazardous location of outcrops. A summary of the sample locations, depths, positions on terrace etc. is presented in Table S1 and sites are marked on Fig. S2. Preliminary studies into the mineralogy of the terrace samples (i.e. XRF analysis) indicated an almost complete absence of potassium feldspar grains and hence focus was placed on the use of quartz OSL.

Two samples (Tab-5 and Tab-16) were too coarse to provide sufficient medium sand for dating. The remaining 21 samples were sieved (180–250 μm) and processed using standard techniques (HCl, H_2O_2, heavy liquids and HF) under subdued red/orange light, to give quartz-rich extracts.

OSL measurements used Risø TL/OSL DA-20 readers fitted with single-grain laser attachments (Bøtter-Jensen et al., 2003, 2010; see Section S1 for further details). Dose determinations made use of the single-aliquot regenerative-dose (SAR) procedure (Murray and Wintle, 2000) with a preheat of 260 °C for 10 s determined based on preheat plateau measurements on multi-grain aliquots (see Fig. S3 and Section S2). Standard data rejection criteria (see Section S3) were initially applied but did not improve the data quality (see also Section 3.3).

Environmental dose rates for each sample were estimated using radionuclide concentrations measured using high resolution gamma spectrometry (Murray et al., 1987) on homogenised materials collected at the sample locations (see Section S4). The resulting quartz dose rates are given in Table S2.

3. Luminescence characteristics

3.1. Multi-grain OSL characteristics

Multi-grain SAR OSL measurements were undertaken on all samples. During preliminary measurements 16 samples were discarded due to low saturation levels (e.g. typical $2^*D_0 < 50$ Gy; see Table S1 for discarded samples). The OSL signals of the five remaining terrace samples (Tab-9, Tab-10, Tab-11, Tab-20 and Tab-21) and two modern analogue samples (MA1 and MA2) were all dominated by the fast component. Fig. S3B shows a representative DRC from sample Tab-9 and the inset shows a typical OSL curve. Individual sample average recycling ratios were within 5% of unity (mean 1.012 ± 0.014, n = 7 samples) and recuperation values were on average less than 1% of the equivalent dose. Multi-grain dose recovery tests (Murray, 1996) were satisfactory for all fossil samples (see inset to Fig. S3C), giving an average dose recovery ratio of 0.97 ± 0.02 (n = 46, Fig. S3C) indicating that our SAR protocol can accurately measure a laboratory dose absorbed before any thermal pre-treatment.

3.2. Multi-grain dose determination

Multi-grain aliquots consist of many individual OSL-sensitive grains and due to averaging effects any information about post-depositional mixing or incomplete bleaching is lost (e.g. Olley et al., 1999; Wallinga, 2002). The only meaningful information that can be retrieved from dose distributions derived from large (8 mm) multi-grain aliquots is the average dose – either unweighted, or weighted (e.g. using the Central Age Model, CAM; Galbraith et al., 1999) according to the uncertainties assigned to individual dose. The individual multi-grain unweighted (arithmetic) averages and CAM averages are all consistent within 1 standard deviation (data not shown). The relative over-dispersions (OD, Galbraith et al., 1999) range between 13 ± 4 and 51 ± 9% and, as expected, are completely consistent with the relative standard deviations, i.e. the contribution from counting statistics and curve fitting errors to the relative standard deviation is not detectable. Thus, for multi-grain dose distributions there appears to be no advantage in deriving CAM dose estimates in preference to an average (arithmetic) dose. The equivalent multi-grain doses given in Table S3 are arithmetic mean doses.

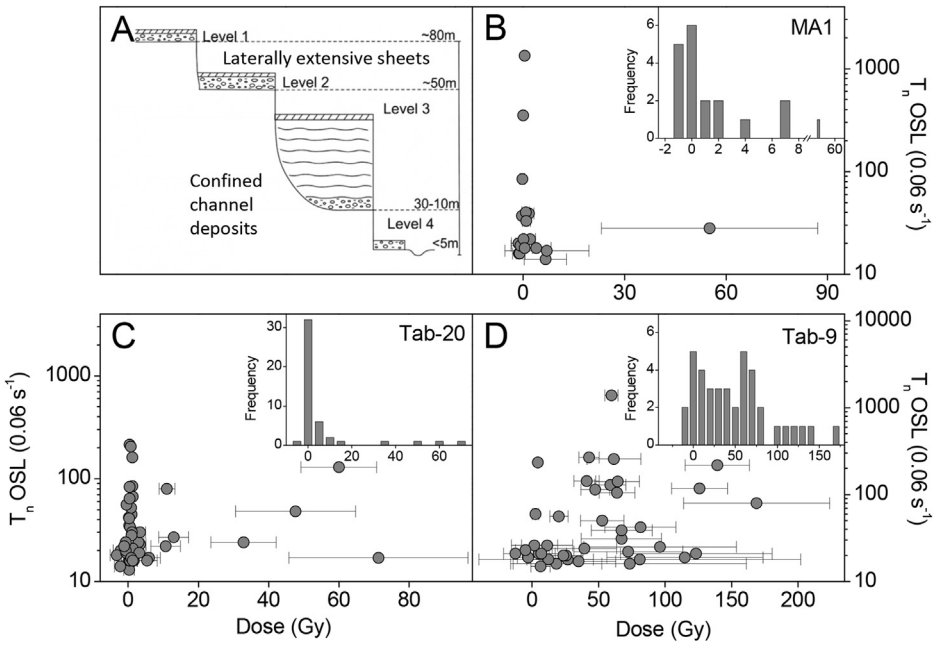

Fig. 1. (A) Schematic cross section of terrace staircase. (B), (C), (D) Natural single-grain quartz dose distributions for (B) the modern analogue (MA1), (C) sample Tab-20 from terrace level 4, and (D) sample Tab-9 from terrace level 3.

3.3. Single-grain OSL characteristics

Single grain measurements show that 98% of the measured grains were rejected because the first (natural) test dose response was undetectable (for test doses of 15 Gy), i.e. $\sigma_{Tn} > 30\%$ (see Section S3); the remaining grains were all relatively dim – the median of the first test dose response in the summation period (first 0.06 s) was only ~1.5 counts/Gy/0.06 s. Applying the remaining single-grain rejection criteria, given in Section S3, resulted in a further reduction in the accepted grain populations by ~20%. However, neither the dose (unweighted arithmetic mean or CAM) nor the relative over-dispersion (OD, Galbraith et al., 1999) changed significantly as a consequence of applying the rejection criteria to the natural and dose recovery dose distributions, i.e. the average ratio of the CAM dose of the dose distribution obtained by using all the rejection criteria and that obtained by only using the $\sigma_{Tn} < 30\%$ criterion is 1.04 ± 0.04 (n = 5 samples). The corresponding ratio for the OD is 1.08 ± 0.08. Thus, it would appear that there is no advantage in applying these standard single-grain rejection criteria for these samples, but there is a cost – the rejection of 20% of otherwise acceptable grains. Similar conclusions have been made by other authors (e.g. Thomsen et al., 2012; Guérin et al., 2015a; Thomsen et al., submitted; Kristensen et al., 2015) for different samples of different origins. Here, we have chosen only to apply the rejection criteria $\sigma_{Tn} < 30\%$ and $L_n/T_n + \sigma_{Ln/Tn} < I_0$.

3.4. Single-grain dose estimation

A single grain is the smallest unit of transport and thus it is generally assumed that information about post-depositional mixing and incomplete bleaching can be extracted from single-grain dose distributions (e.g. Olley et al., 1999; Roberts et al., 2000). It is well-documented that the OSL sensitivity of grains emitting detectable OSL in the response to a laboratory dose varies significantly from one grain to another and typically by several orders of magnitude (e.g. Duller, 2008 and references therein). Thus, the uncertainty assigned to individual dose estimates will also vary considerably and it would seem prudent to weight according to individual uncertainties, although it has been argued that the unweighted arithmetic mean dose may provide a more accurate estimation of age, because the average dose rate is used in age calculations (Guérin et al., 2015b).

In Table S3 and S4 we present single-grain equivalent doses calculated using the unweighted (arithmetic) mean, CAM, CAM unlogged (CAM_{UL}; Arnold et al., 2009) and robust statistics (Tukey, 1977). For single-grain dose distributions CAM is usually the preferred dose estimation model, because it has been argued that CAM is better suited to the statistical properties of such datasets, particularly for older samples (e.g. Arnold et al., 2009). However, the log normal assumption of the CAM prevents the application of this model to the single-grain dose distributions of samples MA1, MA2, Tab-9 and Tab-20, because these contain non-positive dose estimates (see Figs. 1 and S4). Thus, for these samples we cannot apply the CAM without arbitrary rejection of the non-positive dose estimates. Such arbitrary rejection is not required when using the CAM_{UL} or the arithmetic mean. The latter is not widely reported in single-grain studies; mainly because this average can be biased by outlying, poorly known dose estimates. One approach to minimize the effects of outliers is to apply robust statistics to the data sets before calculation of the arithmetic mean. Here, we have arbitrarily but non-subjectively removed outliers identified to be those outside the 1.5 × IQR (InterQuartile Range), where IQR is the difference in dose between the highest and lowest doses remaining after rejection of the lower (0.25) and upper (0.75) quartiles. This approach is the same as that used successfully by Medialdea et al. (2014) for young flash-flood deposits from southeast Spain.

3.5. Single-grain dose recovery and D_0 criterion

Single-grain beta dose recovery tests were undertaken on sample Tab-9 (given dose 15 Gy) and Tab-21 (given doses of either 40 or 60 Gy) and the results are summarised in Table S5. The dose recovery dose distributions are given in Fig. S5. The CAM values for the 40 Gy experiment have been obtained by the arbitrary rejection

of a single non-positive dose estimate (−5 ± 16 Gy). The CAM dose recovery ratios (i.e. measured dose calculated using CAM) for these samples are 1.02 ± 0.04 (n = 83; 15 Gy Tab-9), 0.93 ± 0.07 (n = 35; 40 Gy Tab-21) and 0.76 ± 0.08 (n = 45; 60 Gy Tab-21) with corresponding relative ODs of 15 ± 5%, 27 ± 6% and 59 ± 8% (see Table S5). The average CAM dose recovery ratio is 0.90 ± 0.08 (n = 3). The number of grains rejected due to saturation range between 5 and 14%. These results suggest that our ability to recover a known laboratory dose accurately decreases with increasing dose. Such a trend was also observed by Thomsen et al. (2012).

All these experiments contained grains for which the natural sensitivity corrected signal was in or above saturation of the laboratory dose response and thus no dose estimate could be calculated for these grains (see Table S5). The presence of such grains is a cause for concern as their removal is very likely to involve bias to lower doses. Thomsen et al. (submitted) suggested an alternative rejection criterion which seems to provide an unbiased approach (i.e. independent of the absolute value of individual dose estimates) to the rejection of saturated grains (or grains close to saturation). In this approach the individual D_0 values of all grains are determined and only those dose estimates from grains with a D_0 value equal to or greater than a certain threshold (or cut-off) value, *x*, are accepted; this threshold value *x* is selected to be the same as the average equivalent dose calculated when the rejection criterion is employed. This requires iteration; the threshold value *x* is determined by calculating the average (weighted or unweighted) dose of the dose distribution as a function of *x*. Thomsen et al. (submitted) found that when the threshold value *x* is equal to the average dose of the sample the otherwise unacceptably low dose recovery ratios became acceptable; i.e. for an average sample dose of 60 Gy only grains with a D_0 value larger than 60 Gy are accepted for the next iteration. Then a revised average is calculated and a new threshold set equal to this revised average. This process is repeated until the revised average is equal to or less than the threshold calculated during the previous iteration. By applying this rejection criterion, both Thomsen et al. (submitted) and Guérin et al. (2015a) obtained dose recovery single-grain dose distributions with acceptable CAM dose recovery ratios. In effect, this process rejects those grains for which the DRC saturates at such a low dose that it is unable to record the dose of interest. It is important to note that setting the threshold value too high does not bias the average dose to higher or lower values. It simply increases the random fluctuation in the average value because of the smaller number of accepted grains.

If we now apply the additional rejection criterion to the D_0 values of individual DRCs, then the average CAM dose recovery ratio for all dose recovery experiments increases to 0.97 ± 0.03, the CAM dose recovery ratio at 60 Gy is indistinguishable from unity (i.e. 0.94 ± 0.08) and the number of grains rejected due to saturation reduces to between 0 and 5% (see Table S5). The application of this new criterion appears to have significantly improved our ability to measure a known laboratory dose accurately. The average dose recovery for the arithmetic mean and the IQR average are both acceptable (1.07 ± 0.05 and 0.95 ± 0.03, respectively), whereas the CAM_{UL} average dose recovery ratio is 0.86 ± 0.03, which is not acceptable.

Thomsen et al. (submitted) and Guérin et al. (2015a) applied the D_0 rejection criterion to natural single-grain dose distributions for which the CAM ages underestimated the expected ages based on independent age control and found an improvement in their single-grain ages; it was suggested that this method of analysis reduces a bias towards low doses in the dose distribution by only accepting grains which are able to record the absorbed dose accurately. Since the dose recovery dose distributions of the Tabernas Basin samples suffer from a problem with the inclusion of grains with low D_0 values it is very likely that so will the natural dose distributions. Thus, the effect of this criterion on the natural dose distributions is examined below.

4. Dose distributions and OSL ages

A summary of the multi-grain and single grain quartz OSL doses for the five terrace samples and the two modern analogue samples is presented in Table S3 and S4. Because of the CAM log-normal assumption, this model cannot be applied to the dose distributions obtained for the two modern analogue samples (MA1 and MA2) and samples Tab-9 and -20, all of which contain non-positive dose estimates (see Fig. S4). The CAM dose estimates given in Table S3 and S4 for samples Tab-9 and -20 have been derived after the arbitrary rejection of these non-positive dose estimates. The calculation of the arithmetic mean, IQR and CAM_{UL} doses does not involve any arbitrary rejection of data.

4.1. Modern analogue results

The single-grain dose distributions for the two modern analogue samples are shown in Figs. 1B and S4A (MA1) and S4B (MA2). Both single-grain dose distributions appear to be relatively well-bleached, i.e. the dose distributions are approximately symmetrical with only few “outlying” poorly known dose estimates. If these samples are representative of our fossil deposits then it would clearly be incorrect to employ minimum age models (e.g. MAM, Galbraith et al., 1999) or the finite mixture model (FMM; Galbraith and Green, 1990) to address incomplete bleaching in our older samples. Equally, for these modern analogues it would clearly be incorrect to calculate CAM equivalent dose estimates; rejecting the (legitimate) non-positive dose estimates would lead to a significant bias towards higher doses. The CAM_{UL} single-grain ages are 0.08 ± 0.06 and 0.40 ± 0.14 ka, respectively (see Table S6). Note that the application of the D_0 criterion to these young samples does not result in the rejection of any grains and so the dose distributions remain unchanged. This is because the average equivalent doses are small compared to all measured D_0 values. The arithmetic mean doses are biased by high-dose outliers, but applying the IQR reduces both the average and the variance in the dose distributions; if the IQR is used to reject outliers the CAM_{UL} and average (IQR) ages are consistent with each other.

These modern analogue dose distributions and the resulting ages indicate that incomplete bleaching should not be of significant concern in this environment for samples older than a few thousand years; this is especially true if we remember that modern analogue samples such as these are likely to be worst-case scenarios due to their poor preservation potential (Jain et al., 2004a). These results are also consistent with the review of modern analogue data by Murray et al. (2012).

A priori we would expect average multi-grain doses to agree with average single-grain doses for well-bleached samples. However, the multi-grain ages for these two samples are 2.1 ± 0.8 (MA1) and 5.0 ± 0.5 ka (MA2) and thus overestimate the single-grain ages considerably. Single-grain analysis of sample MA2 showed that 24% of the detectable (i.e. $\sigma_{Tn} < 30\%$) grains were in saturation and thus it is likely that the large discrepancy between the multi-grain and single-grain age for this sample (~4.5 ka) is due to the inclusion of these grains in the multi-grain analysis. The reason why these grains have sensitivity-corrected natural signals in saturation is beyond the scope of this paper, but it is possible that this is a result of the failure of our SAR protocol with these grains. It is interesting to note that similar findings have been reported by Jain et al. (2004b) and Arnold et al. (2012) in their comparisons of single- and multi-grain data.

4.2. Terrace samples

The single-grain dose distributions for the three young samples collected from terrace level 4 (Tab-10, Tab-20 and Tab-21) are shown in Fig. S4C–E. Although, the OD values are high (>60%) these distributions also appear to be relatively well-bleached with only a few outliers at high doses (with the possible exception of Tab-21). This was expected from our modern analogues distributions and suggests that minimum age modelling would be inappropriate. The high dose outliers have no significant impact on the weighted dose estimates (CAM and CAM_{UL}) but do – as expected – affect the arithmetic means. CAM_{UL} and IQR doses are all consistent with each other for these samples except for sample Tab-20. About 17% of the single-grain dose estimates for sample Tab-20 are non-positive and thus the CAM dose given in Table S3 is expected to be too high.

Again the multi-grain ages overestimate the single-grain ages by at least a factor of 2, with CAM_{UL} estimates of between 0.20 ± 0.05 ka (Tab-20) and 2.1 ± 0.2 ka (Tab-21) compared to multi-grain age estimates of 2.0 ± 0.3 ka and 6.4 ± 0.8 ka, respectively. The discrepancy between the multi-grain and single grain ages is again presumably due to the presence of saturated grains (ranging between 10 and 15% of the detectable grain population). Using the D_0 criterion does not change the single-grain ages of these relatively young samples, because all grains have D_0 values larger than 10 Gy.

Fig. S4F and G show the single-grain dose distributions for the two samples from terrace level 3, both of which have ODs of >60%. The dose distribution for sample Tab-9 contains three non-positive dose estimates and thus we cannot apply the CAM (or MAM and FMM) without arbitrary rejection of these dose estimates. For these samples, between 15 and 26% of the grains giving detectable OSL signals (i.e. $\sigma_{TN} < 30\%$) were in saturation (see Table S3). If we apply the D_0 criterion to these samples (see Table S4) the number of grains in saturation is reduced to between 4 and 11%, and the D_e systematically increases by between 1% (CAM_{UL}, IQR) and 53% (CAM).

5. Discussion

In Table S6 both multi-grain and single-grain ages are given for samples Tab-9 and Tab-11, after application of the D_0 rejection criterion. Note that the application of the D_0 criterion only affects the natural dose distributions of the two older samples from terrace level 3. No matter which single-grain dose estimation method is used the multi-grain ages are systematically larger than then the single-grain ages; we attribute this to the significant number of grains in saturation. Thus, the most reliable estimate of burial age is most likely to be derived from the single-grain measurements, where these grains can be identified and eliminated. The CAM_{UL} dose recovery was not consistent with unity (0.86 ± 0.03, n = 3) and so we do not expect these results to be accurate. Although the CAM dose recovery is acceptable (0.97 ± 0.03, n = 3), the CAM cannot be applied to either the modern analogues or two (out of five) of the fossil samples because of the presence of negative doses. Arbitrary rejection of these negative doses would risk biasing any result to larger values. For the three fossil samples where both CAM_{UL} and CAM can be calculated without the arbitrary rejection of non-positive dose estimates the ratio between the CAM_{UL} to CAM is on average 0.76 ± 0.02 (n = 3). The CAM_{UL} measured to given dose ratio in the three single-grain beta dose recovery experiments described above is 0.86 ± 0.03 (after the application of the D_0 criterion, see Table S5), implying that using the CAM_{UL} may lead to significant dose underestimation for these samples and doses (i.e. >15 Gy).

The dose recovery ratio derived using the arithmetic mean is satisfactory (1.07 ± 0.05, n = 3) but the presence of clear outliers in the natural dose distributions makes us question the reliability of these results. In contrast, the "robust statistics" analysis (Tukey, 1977; Medialdea et al., 2014) is the only approach which provides a satisfactory dose recovery (0.95 ± 0.03, n = 3), a non-subjective means of rejecting outliers and can be applied to all samples. Nevertheless, Table S6 summaries the CAM_{UL} ages, the CAM ages after the arbitrary rejection of negative results and the IQR ages (non-subjective rejection of outliers). Not surprisingly, the single-grain arithmetic means are consistently larger than all other analyses, because of the high dose outliers. The CAM_{UL} data for the older two samples ages at the low end of the range and are dismissed because of their poor dose recovery in this dose range. In order to derive the CAM result for one of the oldest samples (Tab-9) three non-positive dose estimates must be arbitrarily rejected. This is likely to produce a bias in the resulting age and it is not surprising that the CAM age of his sample is the oldest of all age estimates. In contrast the CAM result for sample Tab-11 did not involve the arbitrary rejection of non-positive data. Finally, the IQR ages for the two oldest samples are both ~16 ka and are consistent with the presumably more reliable CAM age (19 ± 2 ka) for sample Tab-11.

Turning to the young samples, although the arithmetic mean and CAM tend to give systematically higher ages (with one samples, Tab-20, requiring the rejection of non-positive dose estimates), the CAM_{UL} and the IQR are broadly consistent with each other and clearly indicate deposition through the Mid-to Late-Holocene.

Although this study has been limited by unfavourable luminescence characteristics, the resulting age estimates do add valuable information to the Tabernas Basin stratigraphy. Given terrace level 3 OSL aggradation ages of ~16 ka, it is inferred that deposition of this level occurred during MIS2; this is consistent with the idea of formation under periods of climatic variability suggested by e.g. Macklin et al. (2002). Their suggestion of terrace aggradation during global glacial cycles fits well with regional patterns of terrace formation (Santisteban and Schulte, 2007). Age estimates for terrace level 4 indicate terrace aggradation occurred during the Mid-Late Holocene from 2.8 ± 0.3 ka; although the sample sites on these terraces were buried they were not taken immediately above the base of the terrace sediments and so it is likely that the onset of terrace deposition occurred sometime before this. The abandonment of terrace level 3 at less than ~16 ka provides an older limit to the initiation of terrace level 4. The similarity in age estimates from modern analogue and the youngest terrace level 4 age estimates seems to indicate that this terrace has not yet been completely abandoned; it is presumably still overtopped by large flood events. Our limited chronology is not sufficient to support detailed interpretations of landscape forcing mechanisms; however, it does provide a basis for future geomorphological investigation and application of OSL dating methods in the Tabernas Basin (SE Spain).

6. Conclusions

Quartz OSL dating has been applied to samples derived from a Quaternary fluvial terrace staircase in the Tabernas Basin, SE Spain. Results from single grain dating on modern analogue samples show that signal bleaching is unlikely to be a significant problem for these samples. However, detailed analysis of single grain results shows that measurements from multi-grain aliquots significantly overestimate equivalent doses. This is attributed mainly to the presence of saturated grains. A single-grain D_0 criterion was then applied to data; this criterion is designed to reduce the bias in dose distributions resulting from the use of grains with a small D_0 compared to the expected D_e. When applied to the dose distributions of the two older samples (Tab-9 and Tab-11) the average ages systematically increase, especially when using the CAM. In

summary, although OSL dating was complicated by poor luminescence properties, the findings of this chronological study are consistent with the Harvey et al. (2003) and Harvey (2007) interpretations of landscape response as a result of tectonic base-level changes coupled with patterns of climatic forcing.

Appendix A. Supplementary data

Supplementary data related to this article can be found at http://dx.doi.org/10.1016/j.quageo.2015.05.021.

References

Alexander, R.W., Calvo-Cases, A., Arnau-Roalen, E., Mather, A.E., Lazaro- Suau, R., 2008. Erosion and stabilisation sequences in relation to base level changes in the El Cautivo badlands, SE Spain. Geomorphology 100, 83–90.

Arnold, L., Demuro, M., Ruiz, N., 2012. Empirical insights into multi-grain averaging effects from 'pseudo' single-grain OSL measurements. Radiat. Meas. 47, 652–658.

Arnold, L.J., Roberts, R.G., Galbraith, R.F., DeLong, S.B., 2009. A revised burial dose estimation procedure for optical dating of young and modern-age sediments. Quat. Geochronol. 4, 306–325.

Bailey, R.M., Arnold, L.J., 2006. Statistical modelling of single grain quartz D_e distributions and an assessment of procedures for estimating burial dose. Quat. Sci. Rev. 25, 2475–2502.

Bøtter-Jensen, L., Thomsen, K.J., Jain, M., 2010. Review of optically stimulated luminescence (OSL) instrumental developments for retrospective dosimetry. Radiat. Meas. 45, 253–257.

Bøtter-Jensen, L., Andersen, C.E., Duller, G.A.T., Murray, A.S., 2003. Developments in radiation, stimulation and observation facilities in luminescence measurements. Radiat. Meas. 37, 535–541.

Duller, G.A.T., 2008. Single-grain optical dating of Quaternary sediments: why aliquot size matters in luminescence dating. Boreas 37, 589–612.

Galbraith, R.F., Roberts, R.G., Laslett, G.M., Yoshida, H., Olley, J.M., 1999. Optical dating of single and multiple grains of quartz from Jinmium rock shelter, northern Australia: Part I, experimental design and statistical models. Archaeometry 41, 339–364.

Galbraith, R.F., Green, P.F., 1990. Estimating the component ages in a finite mixture. Nucl. Tracks Radiat. Meas. 17, 197–206.

Geach, M.R., Stokes, M., Telfer, M.W., Mather, A.E., Fyfe, R.M., Lewin, S., 2014. The application of geospatial interpolation methods in the reconstruction of Quaternary landform records. Geomorphology 216, 234–246.

Guérin, G., Frouin, M., Talamo, S., Aldeias, V., Bruxelles, L., Chiotti, L., Dibble, H.L., Goldberg, P., Hublin, J.-J., Jain, M., Lahaye, C., Madelaine, S., Maureille, B., McPherron, S.P., Mercier, N., Murray, A.S., Sandgathe, D., Steele, T.E., Thomsen, K.J., Turq, A., 2015a. A multi-method luminescence dating of the palaeolithic sequence of La Ferrassie based on new excavations adjacent to the La Ferrassie 1 and 2 skeletons. J. Archaeol. Sci. http://dx.doi.org/10.1016/j.jas.2015.01.019.

Guérin, G., Jain, M., Thomsen, K.J., Murray, A.S., Mercier, N., 2015b. Modelling dose rate to single grains of quartz in well-sorted sand samples: the dispersion arising from the presence of potassium feldspars and implications for single grain OSL dating. Quat. Geochronol. 27, 52–65.

Harvey, A.M., 2007. High sinuosity bedrock channels: response to rapid incision – examples in SE Spain. Rev. C&G 21 (3–4), 21–47.

Harvey, A.M., Foster, G., Hannam, J., Mather, A.E., 2003. The Tabernas alluvial fan and lake system, southeast Spain: applications of mineral magnetic and pedogenic iron oxide analyses towards clarifying the Quaternary sediment sequences. Geomorphology 50, 151–171.

Jain, M., Murray, A.S., Bøtter-Jensen, L., 2004a. Optically stimulated luminescence dating: how significant is incomplete light exposure in fluvial environments? Quaternaire 143–157.

Jain, M., Thomsen, K.J., Bøtter-Jensen, L., Murray, A.S., 2004b. Thermal transfer and apparent-dose distributions in poorly bleached mortar samples: results from single grains and small aliquots of quartz. Radiat. Meas. 38, 101–109.

Kristensen, J.A., Thomsen, K.J., Murray, A.S., Buylaert, J.P., Jain, M., Breuning-Madsen, H., 2015. Quantification of termite bioturbation in a savannah ecosystem: application of OSL dating. Quat. Geochronol. 30, 334–341. http://dx.doi.org/10.1016/j.quageo.2015.02.026.

Macklin, M.G., Fuller, I.C., Lewin, J., Maas, G.S., Passmore, D.G., Rose, J., Woodward, J.C., Black, S., Hamlin, R.H.B., Rowan, J.S., 2002. Correlation of fluvial sequences in the Mediterranean basin over the last 200 ka and their relationship to climate change. Quat. Sci. Rev. 21, 1633–1641.

Medialdea, A., Thomsen, K.J., Murray, A.S., Benito, G., 2014. Reliability of equivalent-dose determination and age-models in the OSL dating of historical and modern palaeoflood sediments. Quat. Geochronol. 22, 11–24.

Murray, A.S., Thomsen, K.J., Masuda, N., Buylaert, J.P., Jain, M., 2012. Identifying well-bleached quartz using the different bleaching rates of quartz and feldspar luminescence signals. Radiat. Meas. 47, 688–696.

Murray, A.S., Olley, J.M., 2002. Precision and accuracy in the optically stimulated luminescence dating of sedimentary quartz: a status review. Geochronometria 21, 1–16.

Murray, A.S., Wintle, A.G., 2000. Luminescence dating of quartz using an improved single-aliquot regenerative-dose protocol. Radiat. Meas. 32, 57–73.

Murray, A.S., 1996. Developments in optically transferred luminescence and photo-transferred thermoluminescence dating: application to a 2000-year sequence of flood deposits. Geochim. Cosmochim. Acta 60, 565–576.

Murray, A.S., Marten, R., Johnston, A., Martin, P., 1987. Analysis for naturally occurring radionuclides at environmental concentrations by gamma spectrometry. J. Radioanal. Nucl. Chem. 115, 263–288.

Nash, D.J., Smith, R.F., 2003. Properties and development of channel calcretes in a mountain catchment, Tabernas Basin, southeast Spain. Geomorphology 50, 227–250.

Nogueras, P., Burjachs, F., Gallart, F., Puigdefábregas, J., 2000. Recent gully erosion in the El Cautivo badlands (Tabernas, SE Spain). Catena 40, 203–215.

Olley, J.M., Caitcheon, G.G., Roberts, R.G., 1999. The origin of dose distributions in fluvial sediments, and the prospect of dating single grains from fluvial deposits using optically stimulated luminescence. Radiat. Meas. 30, 207–217.

Porat, N., Amit, R., Enzel, Y., Zilberman, E., Avni, Y., Ginat, H., Gluck, D., 2010. Abandonment ages of alluvial landforms in the hyperarid Negev determined by luminescence dating. J. Arid Environ. 74, 861–869.

Roberts, R.G., Galbraith, R.F., Yoshida, H., Laslett, G.M., Olley, J.M., 2000. Distinguishing dose populations in sediment mixtures: a test of single-grain optical dating procedures using mixtures of laboratory-dosed quartz. Radiat. Meas. 32, 459–465.

Santisteban, J.I., Schulte, L., 2007. Fluvial networks of the Iberian Peninsula: a chronological framework. Quat. Sci. Rev. 26, 2738–2757.

Thomsen, K.J., Murray, A.S., Buylaert, J.P., Jain, M., Hansen, J.H., Aubry, T., 2015. In review. Testing single-grain quartz OSL methods using known age samples from the Bordes-Fitte rockshelter (Roches d'Abilly site, Central France). Quat. Geochronol.

Thomsen, K.J., Murray, A.S., Jain, M., 2012. The dose dependency of the over-dispersion of quartz OSL single grain dose distributions. Radiat. Meas. 47, 732–739.

Tukey, J.W., 1977. Exploratory Data Analysis. Addison Wesley, Reading, Mass.

Vandenberghe, D., Derese, C., Houbrechts, G., 2007. Residual doses in recent alluvial sediments from the Ardenne (S Belgium). Geochronometria 28, 1–8.

Wallinga, J., 2002. Detection of OSL age overestimation using single-aliquot techniques. Geochronometria 21, 17–20.